The post-breakage response of laminated glass with the Gecko® technology

Francesco Freddi[1], Gianni Royer-Carfagni[1], Mirko Silvestri[2]

[1]*Dep. of Civil-Environmental Engineering and Architecture, University of Parma, Italy.*
E-mail: *francesco.freddi@unipr.it, gianni.royer@unipr.it*
[3]*Consorzio Spinner, Bologna, Italy. E-mail*: *mirko.silvestri@gmail.com*

Keywords: Laminated glass, Sentry glass plus SG®, frameless glazing, post-glass-breakage response, fail-safe, point fixing device.

SUMMARY. The *Gecko*® system is a patented innovative point-fixing device of laminated glass for frameless glazing, fully exploiting a new structural ionoplast polymeric interlayer. Here, we record the results of destructive tests performed on laminated panels attached with this system under either wind pressure or dead loads. In the pre-glass-brakeage phase, the panel exhibits a monolithic response confirmed by a full 3D viscoelastic FEM model. The post-glass-brakeage phase has been studied analyzing the cases when either just one or all the glass plies composing the laminated panel are broken. In both cases, glass fragments remain attached to the interlayer after breakage and, consequently, the system can preserve a certain load bearing capacity avoiding sudden collapse (fail-safe response). What is more, even after complete fragmentation of glass, the fixing devices firmly hold the interlayer, which acts as a confining membrane.

1 INTRODUCTION

Glass is the brittle material par excellence. Because of this, any reliable use of this material in architecture cannot neglect that its breakage may be provoked by an imponderable event, like an unfortunate impact at a critical spot or the presence of invisible defects. Hence, it is always necessary to verify that the possible failure of a glass structure does not hurt people or heavily damage properties (fail safe response). An effective technology to achieve structural safety is to bond glass plies together with polymeric sheets *via* a lamination process (laminated glass). The reliability of laminates is in fact associated with the post-glass-breakage performance, i.e., in the ability of the interlayer to maintain coherent the resulting fragments and avoid sudden collapse. The mechanical resistance of the polymeric materials and the glass-polymer adhesion are of primary importance already in the un-cracked stage [1], but even more so in the post-glass-breakage phase.

The post-breakage response of laminated glass is a complex topic, because it is influenced by many factors, such as glass thickness and type (annealed, heat strengthened, tempered), polymeric interlayer (polyvinyl butyral or ionoplast), polymer/glass adhesion, polymer aging, temperature, nature of loading, rate of loading, load duration [2, 3, 4, 5]. In all cases, the fail-safe performance is annihilated if the fixing device of the glass panels is not able to constraint them to the main load bearing structure after glass-breakage. To meet this point, recently an innovative point-fixing device of laminated glass for frameless glazing [6], whose commercial name is *Gecko® system*, has been conceived of, where the interlayer (ionoplastic polymer SG®), slightly extending beyond the edges of the glass plies in proximity of the borders, is bent at right angle and attached to metal clamps directly via the lamination process (figs. 1a-b). The result is an element where the glass

panel is already equipped with metallic winglets, that can be directly connected to any back structure. Remarkably, the interlayer remains attached to the metallic winglets even after complete fragmentation of glass, acting as a confining membrane that preserves the panel integrity.

In a previous study [7], pre- and post-glass-breakage cyclic-tests were performed on reduced scale samples (beams 150mm wide and 500mm long). Three-point-bending tests were conducted on specimens made of different-in-type glass (annealed or thermally tempered), with various levels of artificial ageing in the polymer, at different temperatures (from -20°C to +70°C) and loading rates. The tests confirmed an excellent performance even in the post-glass-breakage phase.

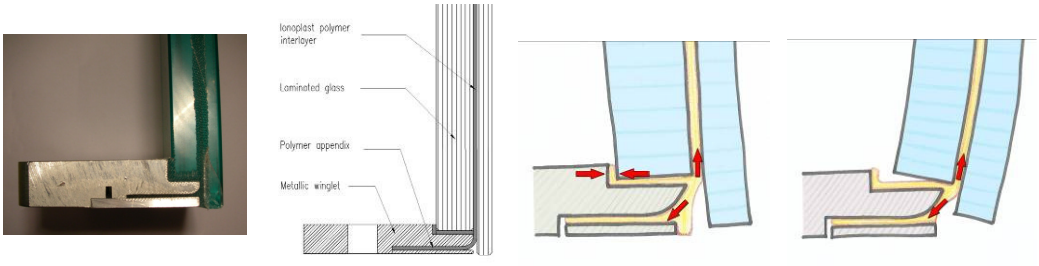

(a) (b) (c) (d)

Figure 1: Lateral view (a) and schematic section (b) of the Gecko® system; (c-d) different constraint of the point-fixing device, corresponding to different load direction.

The aim of this paper is to pursue this research with experiments on full-scale panels. A particular issue to be investigated is: what mechanical constraint is the Gecko® able to offer? The tests on reduced-scale beams [7] clearly evidenced that for actions directed as in fig. 1c, the constraint is a semi-fixed support because a certain bending moment is equilibrated by the couple formed, on the one hand, by the contact force between the upper glass border and the winglet rabbet and, on the other hand, by the resultant of the tensile stress in the polymeric appendix. Differently, when the action is directed as in fig. 1d, only the polymeric interlayer practically equilibrates the pulling action, so that couple reaction is almost negligible and the constraint is practically a hinge. But, besides the particularity of the Gecko® fixing device, the tests here recorded are important to evaluate the bonding action offered in laminated glass by ionoplast interlayers, much less investigated than the traditional PVB. Experimental results have been corroborated by a fully 3D viscoelastic FEM modelling.

Destructive tests have been performed on panels attached with the Gecko® system, evaluating the load bearing capacity and the corresponding deformability when one or both glass plies of the laminated package are broken. In all tests, glass was heat-tempered (this usually shatter in small, square pieces when broken) and loading consisted in the simulation of wind action in a pneumatic chamber, or in the application of dead loads through a water head. Tests have fully confirmed the fail-safe response of the Gecko® attack because the interlayer, remaining attached to the metallic holders, acts as a confining membrane preserving the panel integrity even after complete fragmentation of the glass plies. A certain stiffness and strength are preserved, because the broken pieces of glass, remaining in contact, can withstand compression stress under flexure, while the equilibrating tensile force is carried by the interlayer.

2 RESPONSE OF LAMINATED GLASS UNDER AIR PRESSURE

Laminated heat-tempered glass panels, equipped with 28 resistance strain gages and 4 LVDT transducers, were placed in the large air pressure chamber of fig. 2a under pressures up to ±4.0 kPa (negative value means suction pressure). The Gecko® winglets were slotted and bolted to a metallic frame as in a real façade application. The two lower winglets were constrained as in fig. 2b, so to prevent displacements in the *y* and *z* directions and the rotation around *x*, while in the upper winglets (fig. 2c) the only *z* component of displacement was blocked. To achieve an airtight seal, the gap between the borders of the laminated panel and the contouring frame was filled with 12mm-thick silicone. This, as it will be shown later on, substantially contributed to support the panel at the borders.

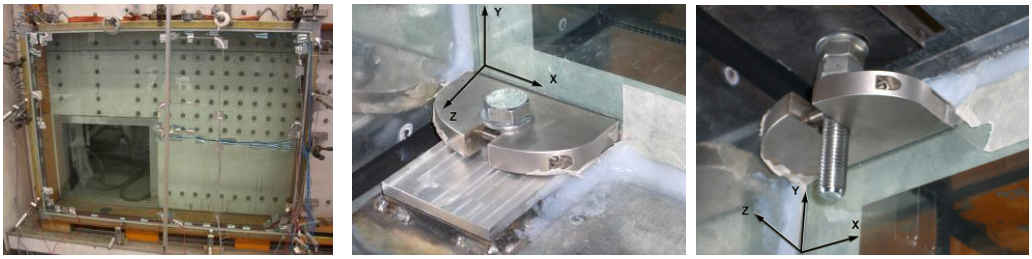

(a) (b) (c)

Figure 2: (a) Experimental apparatus. Detail of the constraint of lower (b) and upper (c) winglets.

Test reference	Glass Condition	Environ. temp.	Load type	Pressure (negative if suction)	Panel Sag at center (mm)
pvg01	Sound	32°C	air	up to +4kPa	+7.8
pvg02	Sound	32°C	air	up to +4kPa	+7.5
pvg03	Sound	32°C	air	up to -4kPa	-7.5
pvg04	Sound	32°C	air	up to +4kPa	+7.3
pvg05	Sound	30°C	air	up to -4kPa	-6.6
pvg06	Sound	30°C	air	up to +4kPa	+6.8
pvg07	Sound	30°C	air	up to -4kPa	-6.3
pvg08	Sound	30°C	air	up to +4kPa	+6.4
pvg09	ext. ply broken	30°C	air	up to +4kPa	+9.6
pvg10	ext. ply broken	30°C	air	up to -4kPa	-8.8
pvg11	both plies broken	30°C	air	up to -1kPa	-11.1
pvg12	both plies broken	30°C	air	up to +2kPa	-
pvg13	both plies broken	30°C	air	up to -2kPa	-
pvg14	both plies broken	30°C	air	up to +3kPa	-
pvg15	both plies broken	30°C	air	up to -3.7kPa	-
pvg16	both plies broken	30°C	air	up to +3.8kPa	+47.8
Pvg17	destructive test	11°C	water	Failure at +4.95kPa	+17.5

Table 1: Test matrix of the experimental program.

The specimens were 1775mm x 1288mm laminated panels, formed by two heat-tempered glass plies (6mm + 12mm) with one 2.28mm ionoplastic interlayer. In each experiment the pressure was gradually augmented until the peak value was reached (Table 1). The maximum chamber pressure

(±4 kPa) could not provoke rupture of the sound panel. Successively, the external (thinner) glass ply was broken with a vanadium chisel and the partially-broken panel tested (fig. 3a). Finally, also the second internal ply was broken, and the response of the completely fragmented panel investigated (fig. 3b). Notice from table 1 that in the latter tests (pvg15 and pvg16) the threshold ±4kPa could not be reached in the air chamber because the broken panel was not any more airtight. Moreover, in tests pvg12-15 the panel deflection exceeded the maximum stroke of the LVDT and the corresponding data could not be recorded. However, in test pvg16 the sag was measured by using a centesimal mechanical comparator. Remarkably, the completely-broken panel could support a considerable pressure (tests pvg15-16), at the price of a deformation of about 50mm.

(a) (b)

Figure 3: Post-glass-breakage tests. Partially broken panel (a) and completely broken panel (b).

The experiments on sound panels were numerically reproduced through a full 3-D FEM model (fig. 4) implemented in ABAQUS [8]. Homogeneous isotropic linear-elastic constitutive equations were used for lime-silica float glass (Young's modulus E = 72 GPa and Poisson's ratio ν = 0.22) and steel winglets (E = 206 GPa and ν = 0.30). The polymer was modeled by a viscoelastic material represented by a generalized series of Maxwell elements, with temperature-dependence considered through the Williams-Landell-Ferry (WLF) theory for the glass-rubber primary transition [9]. Glass and metallic parts were modeled by 8-node solid elements enhanced by incompatible modes: in addition to the displacement degrees of freedom, incompatible deformation modes, variationally deduced from the Hu-Washizu functional, are considered. These additional degrees of freedom eliminate the so-called parasitic shear stress observed in regular displacement elements under bending and the artificial stiffening due to Poisson's effect. Finally, silicone was modelled *à la* Mooney-Rivlin, using the corresponding constitutive law in ABAQUS with parameters C_{01}=0.045 MPa and C_{10}=0.181MPa.

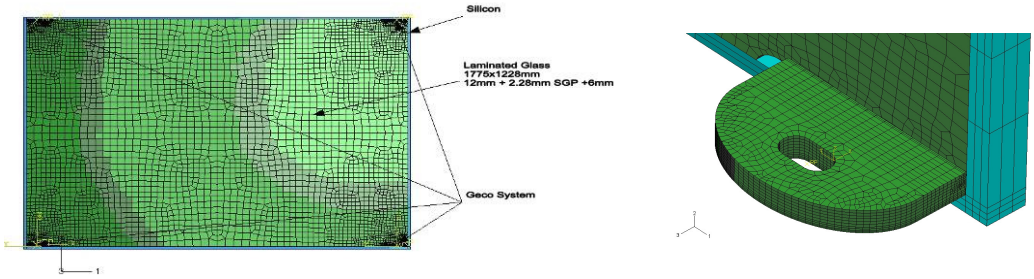

(a) (b)

Figure 4: FEM modelling. (a) Panel mesh; (b) Gecko® device and silicone filler.

2.1 Pre glass-breakage response

The response of a sound panel under positive or negative (suction) pressures is summarized in fig. 5a-b. Notice that the maximum deflection (+6.4mm) under positive pressure (test#pvg08) is slightly larger, in absolute value, than that (-6.3mm) under negative pressure (test #pvg07): this little difference may be due to the asymmetry of the gecko® constraint (see figs. 1b-c). The graphs also show that the results of the FEM simulations are in very good agreement with the experiments. The measured response is slightly non-linear, in part due to the space between bolt and hole at the attacks (figs. 2), in part due to the non-linear (viscoelastic) properties of the polymer.

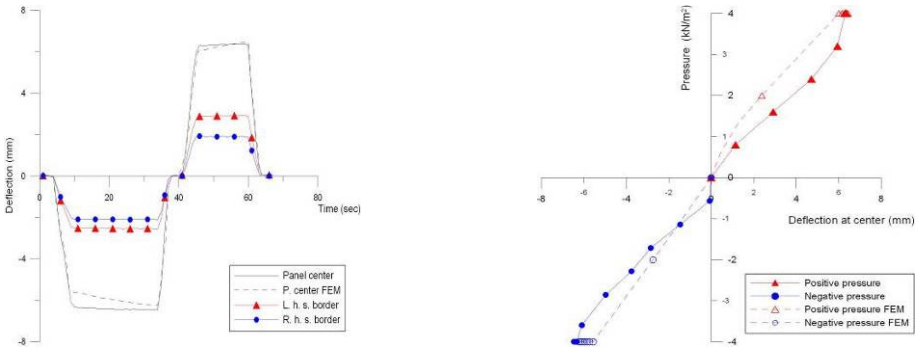

(a) (b)

Figure 5: (a) Displacement vs. time at the panel centre and at the left- and right hand- side borders under negative (suction, test pvg07) and positive pressure (test pvg08). (b) Pressure vs. maximum deflection at panel centre under negative (suction, test pvg07) and positive pressure (test pvg08).

The outputs of the four strain gages placed at the panel centre are reported in figs. 6a and 7a for negative and positive pressures. Strains in *x* and *y* direction at the intrados and extrados of the panel are practically equal in absolute value for negative and positive pressure. This is confirmed by figs. 6b and 7b that represent the stress components σ_{xx} and σ_{yy} through panel-thickness under negative pressure, calculated *via* the FEM code. The monolithic response is evidenced by matching curvatures of both plies composing the laminate.

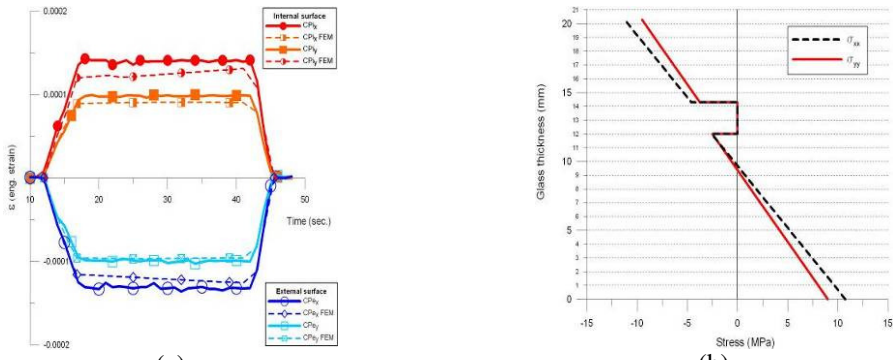

(a) (b)

Figure 6: Negative pressure test (pvg07): (a) experimental strain vs. time at the panel centre; b) stress in the laminate thickness obtained *via* FEM.

The comparison between the measured strains and the FEM simulations has evidenced the important structural role played by the silicone sealant, usually neglected in the calculations. At maximum pressure (4kPa) the Gecko® winglets carry only 60% of the applied load, whereas the remaining portion is transferred through the silicone layer. Keeping the loads constant, the load carried by the Gecko® decreases of a further 11%, probably because of the viscosity of the polymeric interlayer. In general, the numerical model gives very accurate results, although it slightly underestimates (difference less than 5%) the measured strains.

Notice that the positive- and negative-pressure cases are practically symmetric. This indicates that the asymmetry of the Gecko® constraint (figs. 1b-c), which was evident in the tests on laminated beams [7], is negligible in the 2-D case of laminated panels. The deformed shape is anticlastic in a neighborhood of the geckos, due perhaps to the presence of the silicone layers.

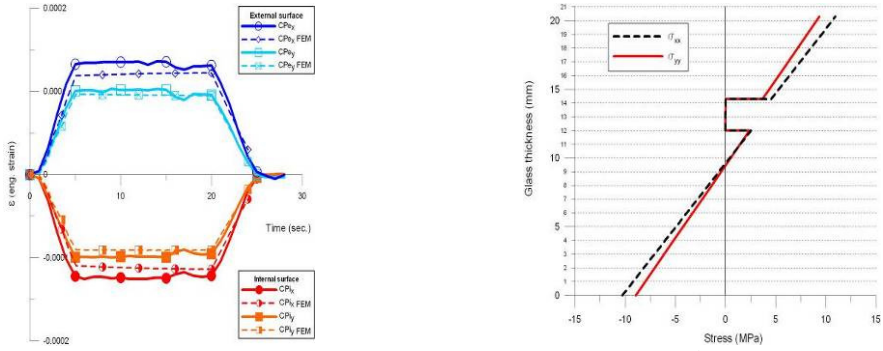

(a) (b)

Figure 7: Positive pressure (test pvg08): (a) strain vs. time at the panel centre; b) stress in the laminate thickness obtained *via* FEM.

2.2 Response with the external glass ply broken

In a second series of tests, the external (6mm-thick) ply of the laminated panel was broken before loading (fig. 9a). The glass shattered into large pieces (diameter ~100mm), perhaps indicating an incomplete tempering, that remained attached to the underlying polymeric sheet.

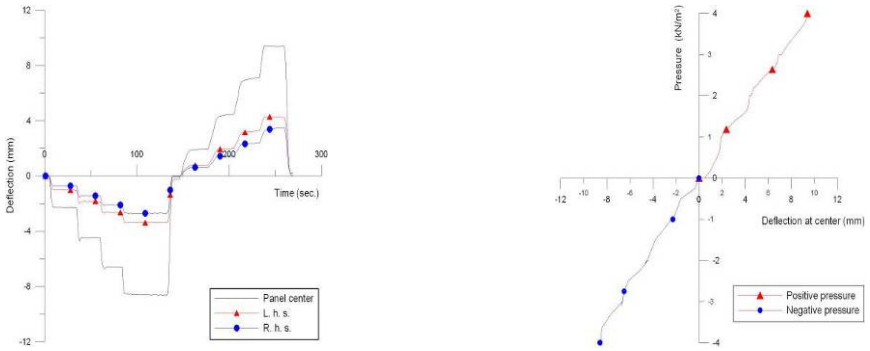

(a) (b)

Figure 8: Laminated panel with broken external ply. (a) Displacement vs. time at the panel centre and at the borders under negative (test pvg10) and positive pressure (test pvg09). (b) Pressure vs. deflection at panel centre under negative (test pvg10) and positive pressure (test pvg09).

Fig. 8 represents the displacement measured by LVDTs under negative and positive pressures (gradually increased at steps of ±1 kPa up to ±4 kPa, maintaining it constant for ~25 sec after each step). Notice that the maximum deflection under positive pressure (+9.6mm, test #pvg09) is higher (in absolute value) than under negative pressure (-8.8mm, test #pvg10). In fact, in the second case the external glass ply tends to be compressed and can carry a certain load due to the direct contact of the glass fragments (fig. 9b). The deflection is higher than that of a sound panel (~6.3mm), but much less than the deflection of one 12mm ply (~20mm). Under positive pressures, the broken ply still contributes to the overall stiffness of the panel because the attached glass fragments produce the tension stiffening of the polymeric sheets that reinforce the sound ply (fig. 9c). The deformed shape is qualitative similar to that of a sound panel, but in proximity of the Gecko® attacks the deformed surface from anticlastic becomes synclastic as the pressure level is augmented.

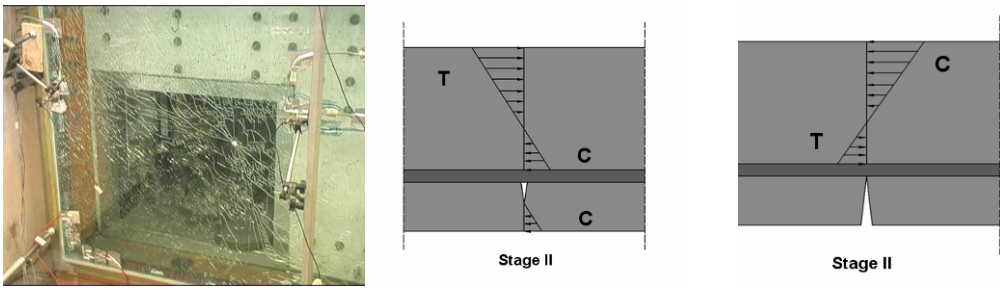

(a) (b) (c)

Figure 9: (a) Panel with broken external ply; stress under negative (b) and positive (c) pressures.

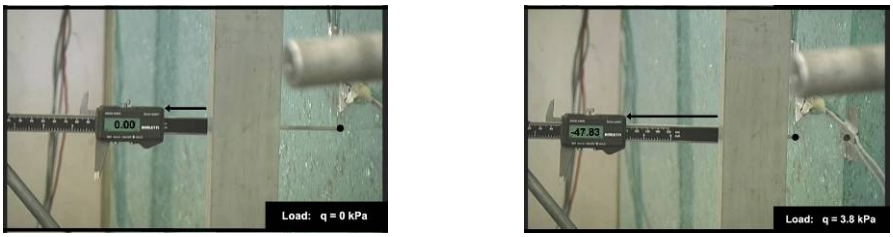

(a) (b)

Figure 10: Broken laminated panel. Measured sag (a)→(b) under positive +3.8 kPa pressure.

2.3 Response with both glass pies broken

In the third test series also the internal (12mm) ply was broken (fig. 12a). The size of resulting fragments was again around 10cm, indeed quite large for a heat-tempered glass. The panel was subjected to various pressure levels, both negative and positive (tests pvg11-16), up to -3.7 kPa and +3.8 kPa. The measured deflection at the centre was so high to exceed the maximum stroke of the applied LVDTs (10mm). The measure was then manually taken with a vernier caliper and, under maximum pressure, it was found to be 47.83mm at the panel centre (figs. 10a-b). The maximum deflection at the panel borders, which remained within the range of the 10mm stroke of the LVDTs and could be recorded, is represented in Fig. 11. Notice that in general the deflection is a non-linear function of the pressure and it is comparable (in absolute value) for negative and positive pressures. Due to the higher deformability of the broken panel, its deformation in a neighborhood of the Gecko® devices was, in general, anticlastic.

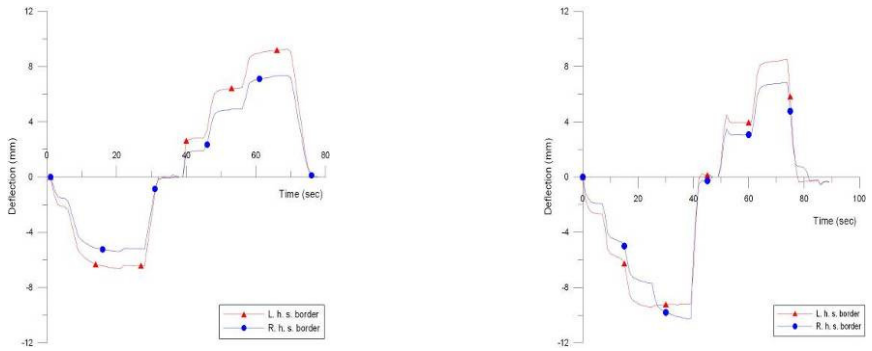

(a) (b)

Figure 11: Displacement vs. time at the borders of a completely broken panel. (a) Deflection under negative (−2kPa, test pvg13) and positive pressures (+3kPa, test pvg14). (b) Deflection under negative (−3.7kPa, test pvg15) and positive pressure (+3.8kPa, test pvg16).

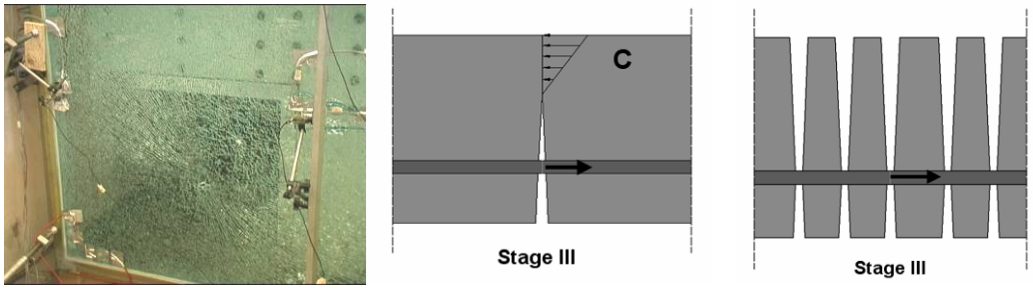

(a) (b) (c)

Figure 12: (a) Broken panel; (b-c) Different load-bearing schemes.

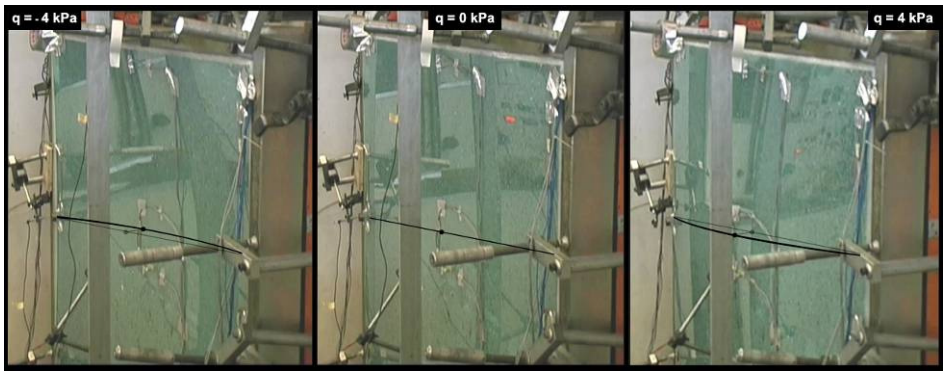

Figure 13: Large deformation and membrane effect of polymeric interlayer in broken panels.

Remarkably, even with both glass plies broken, the panel was able to support pressures of the order of ±4kPa. The ionoplast-polymeric interlayer remained fastened to the metallic winglet to form a retaining membrane under tensile stress. The measured strains have evidenced that two structural schemes contribute, in parallel, to withstand the applied actions: *i*) a certain flexural

stiffness is maintained by the internal couple formed by the compressive stresses of one glass ply (from direct contact of the broken fragments) and the tensile stresses in the polymeric interlayer, stiffened by the fragments of the second ply (fig. 12b); *ii*) the large deformation of the panel, with the considerable curvature that derives, allows for the establishment of membrane stresses in the interlayer that balances a quote of the pressure acting orthogonally to the surface (fig. 12c). This second scheme becomes more and more important with increasing loads, and can be established if and only if the interlayer remains attached to the holders after glass breakage (fig. 13). Moreover, there is the beneficial presence of silicone sealants at the borders, whose role was far from being negligible in the pre-glass-breakage phase, but even more so in the post-glass-breakage phase, when the deformation considerably increases.

3 RESPONSE OF LAMINATED GLASS UNDER DEAD LOADS

To assess the response against permanent loads (e.g., snow), another laminated panel was placed horizontally (the Gecko® winglets directed upward) and metallic sheets were fastened all around the fixing frame so to form a tank (fig. 14) to be filled up with water. The specimen was a 1478mm x 1450mm two-ply laminated (8 + 1.52 + 6mm) panel. Environmental temperature was +10°C, and no silicone sealant was used to fill the gap between the glass borders and the contouring frame. Indeed, a large delamination was observed already in the unstressed panel that, because of this, should have been rejected if it had to be used in a building. However, its testing was of interest to evaluate the ultimate response of a defective element.

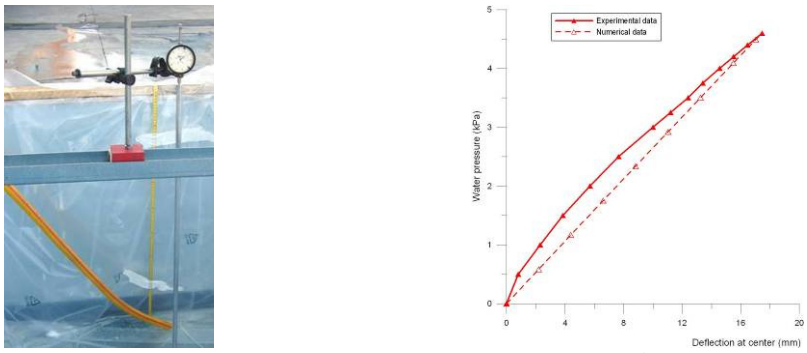

(a) (b)

Figure 14: Tests with water head. (a) Dial gage to measure the sag at panel center. (b) Water pressure (kPa) vs. deflection (mm) at panel centre.

3.1 Pre glass-breakage response and failure mechanism

The tests were conducted by measuring the height of the water head as the tank was filled up and the deflection in the panel centre (fig. 14a). The graph pressure vs. deflection (test #pvg17) is represented in Fig. 14b. The speed of the applied load was approximately 0.0054kPa/sec and the panel failed after approximately 15 minutes, when the water head was about 46 cm. Summing up the contributions from water (4.6 kPa) and panel dead-weight (0.35 kPa), failure pressure for this test was 4.95 kPa. The corresponding deflection, not considering the initial sag due to the panel dead weight, was 17.45mm. The graph is sensibly linear, apart from a little disturbance at the origin, probably due to the settling of the panel. The measured response was in agreement with the results of Section 2. Substantial differences were only observed in the measured strain at those

Gecko® attacks where glass was delaminated (fig. 15a). Here, the glass ply not directly loaded (the external one) remained practically stress free, whereas the other ply (the internal) carried the whole actions deforming anticlastically.

(a) (b) (c)

Figure 15: Panel under water load. (a) Initial delamination; (b-c) rupture at delaminated corners.

The test was clearly stress-driven: the critical stage is consequently quite different from the tests with air pressure discussed in Section 2, where panels were first loaded and then pressurized. Failure was sudden and immediate. Recording with a digital camera has evidenced that it was the internal (8mm-thick) glass ply to break first because overloaded in a neighborhood of the delaminated corned (fig. 15a). Then, also the external ply fragmented and, immediately after, the polymeric interlayer fractured in proximity of the four Gecko devices. Therefore, collapse was not triggered by the premature crisis of the attack but by rupture of the taut glass ply. With both plies broken, the main load-bearing mechanism was offered by the membrane effect of the polymeric interlayer. However, in proximity of the Gecko® devices the stress in the ionoplast interlayer overcame its strength and provoked the sudden separation of the panel from the fixing devices; hence, the rupture of the second ply and the overloading of the interlayer membrane with its eventual rupture. The polymer never detached from the metallic winglet but simply got torn at the critical sections provoking the separation from supports (figs. 15b-c). Remarkably, the resistance of the Gecko® attack was not diminished by possible defects such as delamination.

4 DISCUSSION. SAFE-LIFE VS. FAIL-SAFE.

The tests under air pressure (Section 2) and water pressure (Section 3), are correlated with two different but complementary approaches to the design of glass structures, and usually referred to as "safe-life" and "fail-safe" design. In *safe-life design* products are designed to survive a specific design life with a chosen reserve. This technique is employed in critical systems which are either very difficult to repair or may cause severe damage: such systems are designed to work for years without requirement of any repairs. Complementary to this is the *fail-safe design*, the approach conceiving devices which, if or when they fail, will cause a minimum of harm.

The tests under increasing water head (Section 3) interpret the approach of safe-life design because they allow to evaluate the strength of the panel under quasi-static monotonic loading and, consequently, the safety factor under design loads. In this case rupture is sudden and violent, triggered by failure of one of the glass plies rather than by premature crisis of the Gecko® attacks: the first fracture of one of the plies produces a chain reaction which implies, in sequence, the rupture of the second ply and the overloading of the interlayer membrane with its eventual rupture. The gecko® attack performed extremely well, because the polymer never detached from the metallic winglet but simply got torn at the critical sections, provoking the separation of the panel from the supports. The system also proved to be *robust*, because the resistance of the Gecko® was

not diminished by possible defects such as delamination. Consequently, the Gecko® system proved to possess sufficient reserve to safely endure over the years under design load.

On the other hand, the tests of Section 2 accord with the fail-safe design approach because they represent the possible scenario of a panel broken by an imponderable event, such as an accidental impact, and what is investigated is the residual load-bearing-capacity after this event. The structure fixed with the gecko® devices showed an excellent response due to the noteworthy post-glass-breakage performance, enhanced by the high mechanical properties of ionoplast polymers.

The fail-safe approach is by far inalienable. In fact, it can never be excluded, for example, that the fortuitous impact of a sharpened body may provoke partial or full rupture of a laminated panel: in this case it is fundamental to verify that the element does not fall down under permanent and, say, wind loads. This is much more important than controlling the structural strength under applied loads that exceed the maximum design values and remain constant for a time sufficient to provoke the collapse of the structure.

Last but not least, the tests have shown that the silicone sealants, whose effect is always neglected in the design practice, may instead give a substantial contribution to the load bearing capacity, especially in the post-glass breakage phase, thus increasing the fail-safe performance.

References

[1] Bennison, S. J., Jagota, A. and Smith, C. A., "Fracture of glass/polyvinyl butyral (Butacite) laminates in biaxial flexure", *Journal of the American Ceramic Society*, **82**(7), 1761-1770 (1999).

[2] Pantelides, C. P., Horst, A. D. and Minor, J. E., "Post-breakage behavior of architectural glazing in Windstorms", *Journal of Wind Engineering and Industrial Aerodynamics*, **44**, 2425-2435 (1992).

[3] Pantelides, C. P., Horst, A. D. and Minor, J. E., "Post-breakage behavior of heat strengthened laminated glass under wind effects", *J. of Structural Engineering ASCE*, **119**, 454 467 (1993).

[4] Beason, W. L. and Morgan, J. R., "Glass failure prediction model", *J. of Structural Engineering ASCE*, **110**, 197-212 (1984).

[5] Seshadri, M., Bennison, S. J., Jagota, A. and Saigal, S., "Mechanical response of cracked laminated plates", *Acta Materialia*, **50**, 4477-4490 (2002).

[6] Frambati, F. and Royer-Carfagni, G. (Inventors), "Stratified flat element with intermediate layer extended and folded beyond at least one perimetral edge of the said flat element", *European Patent dep. n. 05075628.7* (2005).

[7] Royer-Carfagni, G. and Silvestri, M., "Fail-safe point fixing of structural glass. New advances", *Engineering Structures*, **31**, 1661-1676 (2009).

[8] *ABAQUS version 6.5*, Hibbit, Karlsson & Soresen, Inc., Pawtucket, R.I., USA (2005).

[9] Ferry, J. D., *Viscoelastic Properties of Polymers*, 3rd edition, John Wiley & Sons (1980).